Monatshefte für Chemie 138, 819–822 (2007)
DOI 10.1007/s00706-007-0702-6
Printed in The Netherlands

Monatshefte für Chemie
Chemical Monthly

Rare Earth-Rich Indides $RE_5Pt_2In_4$ (RE = Sc, Y, La–Nd, Sm, Gd–Tm, Lu)

Roman Zaremba, Ute Ch. Rodewald, and **Rainer Pöttgen***

Institut für Anorganische und Analytische Chemie, Westfälische Wilhelms-Universität Münster, Münster, Germany

Received February 22, 2007; accepted April 20, 2007; published online July 5, 2007

Summary. The isotypic indides $RE_5Pt_2In_4$ (RE = Sc, Y, La–Nd, Sm, Gd–Tm, Lu) were synthesized by arc-melting of the elements and subsequent annealing. They were investigated *via* X-ray powder diffraction. Small single crystals of $Gd_5Pt_2In_4$ were grown *via* slow cooling and the structure was refined from X-ray single crystal diffractometer data: *Pbam*, $a = 1819.2(9)$, $b = 803.2(3)$, $c = 367.6(2)$ pm, $wR^2 = 0.089$, 893 F^2 values and 36 parameters. The structure is an intergrowth variant of distorted trigonal and square prismatic slabs of compositions GdPt and GdIn. Together the platinum and indium atoms build up one-dimensional $[Pt_2In_4]$ networks (292–333 pm Pt–In and 328–368 pm In–In) in an AA stacking sequence along the c axis. The gadolinium atoms fill distorted square and pentagonal prismatic cages between these networks with strong bonding to the platinum atoms.

Keywords. Rare Earth Compounds; Indides; Crystal Chemistry.

Introduction

Within the large series of $RE_xT_yIn_z$ indides (RE = rare earth element, T = transition metal), the systems with 5*d* metals have only scarcely been investigated [1]. Most data are available for the platinum and gold based systems, however, only with respect to the transition metal- and indium-rich parts of the phase diagrams, where compounds with $[T_yIn_z]$ polyanions exist. The rare earth-rich part has only been investigated in more detail for the Ce–Pt–In system. The structures of the indides Ce_2Pt_2In [2], $Ce_{12}Pt_7In$ [3], and $Ce_5Pt_2In_4$ [4] have been reported. In the three structures, the cerium atoms have high coordination numbers between CN 12 and 17 with a large variety of Ce–Ce interactions (322–414 pm Ce–Ce).

We have now extended our phase analytical studies on the rare earth-rich parts of the other RE–Pt–In systems. Herein we report on the syntheses and structural characterization of the indides $RE_5Pt_2In_4$ (RE = Sc, Y, La–Nd, Sm, Gd–Tm, Lu) with orthorhombic $Lu_5Ni_2In_4$ type structure [5].

Discussion

New rare earth metal rich indides $RE_5Pt_2In_4$ (RE = Sc, Y, La–Nd, Sm, Gd–Tm, Lu) crystallize with the orthorhombic $Lu_5Ni_2In_4$ type [5] structure. The latter type has also been observed for $Sc_5Ni_2In_4$ and $Sc_5Rh_2In_4$ [8] as well as for $Zr_5Rh_2In_4$ and $Hf_5Rh_2In_4$ [10]. As expected from the lanthanoid contraction, the cell volume within the $RE_5Pt_2In_4$ series continuously deceases from the lanthanum to the lutetium compound (Fig. 1). Due to the larger size of platinum with respect to nickel, the $RE_5Pt_2In_4$ indides show slightly higher cell volumes as compared to the isotypic $RE_5Ni_2In_4$ series [5]. The cell volume of $Y_5Pt_2In_4$ fits in between the volumes of $Tb_5Pt_2In_4$ and $Dy_5Pt_2In_4$, as frequently observed for such rare earth-transition metal-indides [1]. The by far smallest cell volume was observed for $Sc_5Pt_2In_4$ (Table 1). Since we have observed superstructure formation for $Zr_5Ir_2In_4$ [11] upon doubling the subcell c axis, we have carefully checked the *Guinier* powder pattern of the scandium compound, however, there was no indication for additional reflections. The small negative anomaly for $Ce_5Pt_2In_4$ can most

* Corresponding author. E-mail: pottgen@uni-muenster.de

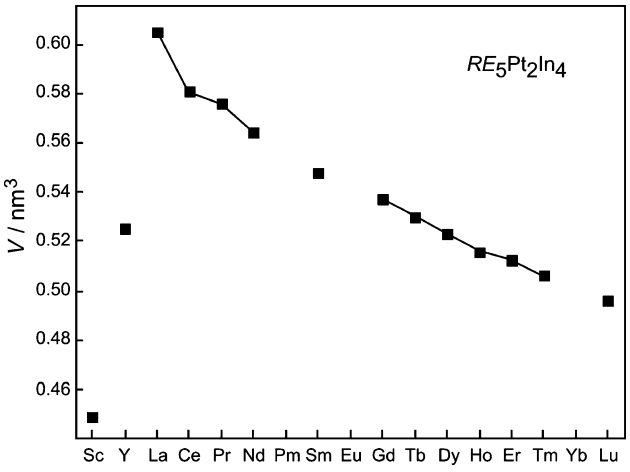

Fig. 1. Plot of the cell volumes of the $RE_5Pt_2In_4$ indides

Table 1. Lattice parameters (*Guinier* powder data) of the ternary indium compounds $RE_5Pt_2In_4$

Compound	a/pm	b/pm	c/pm	V/nm^3
$Sc_5Pt_2In_4$	1743(1)	765.2(6)	336.8(2)	0.4491
$Y_5Pt_2In_4$	1806.2(5)	800.6(3)	363.3(1)	0.5254
$La_5Pt_2In_4$	1875.2(6)	833.9(3)	387.0(1)	0.6051
$Ce_5Pt_2In_4$	1856.3(9)	819.0(6)	382.0(2)	0.5808
$Ce_5Pt_2In_4$*	1857.9(4)	820.88(14)	381.88(8)	0.5824
$Pr_5Pt_2In_4$	1854(2)	818.3(5)	379.6(2)	0.5758
$Nd_5Pt_2In_4$	1842(2)	814.3(7)	376.0(3)	0.5641
$Sm_5Pt_2In_4$	1827.3(9)	807.6(4)	371.2(1)	0.5478
$Gd_5Pt_2In_4$	1819.2(9)	803.2(3)	367.6(2)	0.5371
$Tb_5Pt_2In_4$	1811(2)	802.0(5)	364.7(2)	0.5299
$Dy_5Pt_2In_4$	1804(1)	798.8(4)	363.0(2)	0.5232
$Ho_5Pt_2In_4$	1803(1)	794.6(1)	360.1(1)	0.5157
$Er_5Pt_2In_4$	1794.5(6)	794.4(4)	359.45(9)	0.5124
$Tm_5Pt_2In_4$	1788(1)	792.1(6)	357.6(3)	0.5064
$Lu_5Pt_2In_4$	1778.5(5)	787.3(2)	354.4(1)	0.4962

* Data from Ref. [4]

likely be attributed to a tendency of cerium for an intermediate valent state. Similar behavior has also been observed for other series of rare earth metal based indides [1]. Physical property investigations on the $RE_5Pt_2In_4$ indides are planned in order to clarify the volume anomaly.

The main features of crystal chemistry of $Lu_5Ni_2In_4$ type indides has been discussed in detail in the previous papers [4, 5, 8, 10, 11]. Therefore, herein we focus only on the peculiarities of the platinum series $RE_5Pt_2In_4$. First, the platinum based series exists for the whole range of rare earth elements, except divalent europium and ytterbium, while the $RE_5Ni_2In_4$ nickel indides have been observed only for the smaller rare earth elements.

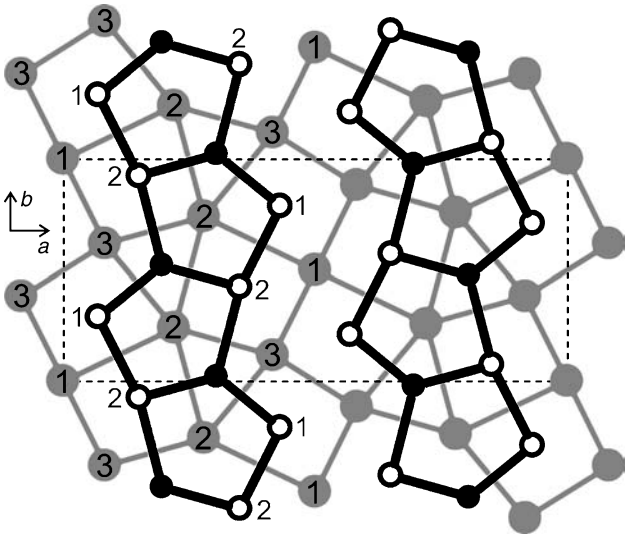

Fig. 2. Projection of the $Gd_5Pt_2In_4$ structure onto the *xy* plane. Gadolinium, platinum, and indium atoms are drawn as gray, filled, and open circles. All atoms lie on mirror planes at $z = 0$ (thin lines) and $z = 1/2$ (thick lines). The $[Pt_2In_4]$ networks and the trigonal and square prismatic slabs build up by the gadolinium atoms are emphasized

As shown in Fig. 2 for $Gd_5Pt_2In_4$, the structure is a simple intergrowth of slightly distorted platinum, respectively indium filled trigonal and square prisms. The platinum and indium atoms build up $[Pt_2In_4]$ networks. In $Gd_5Pt_2In_4$ each platinum atom has two nearer (292 and 297 pm) and one longer (333 pm) indium neighbor. All of these Pt–In distances are longer than the sum of the covalent radii of 279 pm [12]. Even for the shorter Pt–In distances we can assume only weaker Pt–In bonding. Ternary indides with strong Pt–In bonds (high crystal orbital overlap populations) like $SrPtIn_2$ [13] or $BaPtIn_2$ [14] show Pt–In distances close to the sum of the covalent radii.

The smaller $[PtIn_2]$ units are connected *via* a shorter In1–In2 distance of 328 pm leading to the $[Pt_2In_4]$ network. These In–In distances compare well with elemental indium (tetragonally distorted *fcc* variant), where each indium atom has four neighbors at 325 pm and additionally eight neighbors at 338 pm [15]. The shortest In–In distance between the $[Pt_2In_4]$ networks (421 pm In1–In1) is much longer, and therefore the networks have a pronounced one-dimensional character.

The shortest interatomic distance in $Gd_5Pt_2In_4$ occurs for Gd3–Pt (286 pm), even slightly smaller than the sum of the covalent radii of 290 pm [12]. We can thus assume strong Gd–Pt bonding in $Gd_5Pt_2In_4$.

Similar Gd–Pt distances have also been observed in $Gd_3Pt_4In_{12}$ (299 and 302–pm) [16].

Within the gadolinium network (tessellation of distorted triangles and squares) we observe shorter Gd1–Gd3 (342 pm) and Gd3–Gd3 (357 pm) distances. Each gadolinium atom has a further gadolinium neighbor at 367 pm Gd–Gd, the latter distance corresponds to the *c* axis. All of these Gd–Gd distances compare well with the average Gd–Gd distance of 360 pm in *hcp* Gd [15]. Besides strong Gd–Pt bonding, also Gd–Gd bonding significantly contributes to the stability of $Gd_5Pt_2In_4$.

Experimental

Synthesis

Starting materials for the preparation of the $RE_5Pt_2In_4$ indides were ingots of the rare earth metals (Johnson Matthey, Chempur or Kelpin), platinum powder or granules (Degussa-Hüls or Heraeus), and indium tear drops (Johnson Matthey), all with stated purities better than 99.9%. In a first step, the rare earth metal pieces were melted under 600 mbar argon to small buttons in an arc-melting furnace [6]. The argon was purified over titanium sponge (900 K), silica gel, and molecular sieves. The pre-melting procedure reduces shattering during the subsequent reactions with platinum and indium. The rare earth metal buttons were then mixed with cold-pressed pellets (Ø 6 mm) of platinum and pieces of the indium tear drops in the atomic ratio 46:18:36, reacted in the arc-furnace and remelted three times to ensure homogeneity. Alternatively, the samples can also be prepared by induction melting of the elements. The weight losses after the melting procedures were always smaller than 0.5%. The light gray polycrystalline samples are brittle and stable in air over months. Finely ground powders are dark gray and single crystals exhibit metallic luster.

Scanning Electron Microscopy

The single crystal investigated on the diffractometer has been analyzed by EDX measurements using a LEICA 420 I scanning electron microscope with GdF_3, platinum, and InAs as standards. Since the crystal was mounted by beeswax on a glass fibre, it was first coated with a thin carbon film. No impurity elements were detected. The experimentally observed composition (44 ± 2 at-% Gd : 20 ± 2 at-% Pt : 36 ± 2 at-% In) was in good agreement with the ideal composition (45.5 : 18.2 : 36.3).

X-Ray Film Data and Structure Refinement

The $RE_5Pt_2In_4$ indides were characterized by X-ray powder diffraction using a Nonius FR 552 *Guinier* camera with Cu Kα_1 radiation and α-quartz ($a = 491.30$, $c = 540.46$ pm) as an internal standard. The camera was equipped with an imaging plate system (Fujifilm BAS-1800). The lattice parameters (Table 1) were deduced from least-squares fits of the powder data. The correct indexing was ensured through intensity calculations [7], taking the atomic positions obtained from the structure refinement. For $Ce_5Pt_2In_4$ the lattice parameters are in agreement with the data given in Ref. [4].

Table 2. Crystal data and structure refinement for $Gd_5Pt_2In_4$ ($Lu_5Ni_2In_4$ type, *Pbam*, Z=2)

Molar mass	1635.71 g/mol
Calculated density	10.11 g/cm^3
Crystal size	$10 \times 15 \times 40\ \mu$m^3
Detector distance	60 mm
Exposure time	40 min
ω range; increment	0–180°, 1.0°
Absorption coefficient	64.5 mm^{-1}
Integr. param. A, B, EMS	13.0, 2.3, 0.024
$F(000)$	1344
Transm. ratio (max/min)	1.23
θ range	3°–30°
Range in *hkl*	±25, ±11, ±5
Total no. reflections	5169
Independent reflections	893 ($R_{int} = 0.135$)
Reflections with $I > 2\sigma(I)$	688 ($R_\sigma = 0.084$)
Data/parameters	893/36
Goodness-of-fit on F^2	1.265
Final R indices [$I > 2\sigma(I)$]	$R^1 = 0.069$
	$wR^2 = 0.085$
R indices (all data)	$R^1 = 0.094$
	$wR^2 = 0.089$
Extinction coefficient	0.00039(8)
Largest diff. peak and hole	4.01/−4.45 e/Å^3

Most of the $RE_5Pt_2In_4$ samples were polycrystalline. Only in the $Gd_5Pt_2In_4$ sample we found small crystals. The latter were examined by *Laue* photographs on a *Buerger* precession camera (equipped with an imaging plate system Fujifilm BAS-1800) in order to establish suitability for intensity data collection. The data set of the $Gd_5Pt_2In_4$ crystal was collected in oscillation mode on a *Stoe* IPDS-II image plate diffractometer using monochromatized Mo Kα radiation (71.073 pm). Due to the small crystal size and the weak scattering power, an irradiation time of 40 min was used. A numerical absorption correction was applied to the data set. All relevant crystallographic details for the data collection and evaluation are listed in Table 2.

The systematic extinctions of the data set were compatible with space group *Pbam*. The isotypy of the $RE_5Pt_2In_4$ indides

Table 3. Atomic coordinates and isotropic displacement parameters (pm^2) of $Gd_5Pt_2In_4$, space group *Pbam*. U_{eq} is defined as one third of the trace of the orthogonalized U_{ij} tensor

Atom	*Wyck.*	x	y	z	U_{eq}
Gd1	2*a*	0	0	0	126(4)
Gd2	4*g*	0.22059(8)	0.2413(2)	0	116(3)
Gd3	4*g*	0.41693(8)	0.1180(2)	0	107(3)
Pt	4*h*	0.30429(6)	0.0230(2)	1/2	106(3)
In1	4*h*	0.5691(1)	0.2105(3)	1/2	128(5)
In2	4*h*	0.8501(1)	0.0751(3)	1/2	143(4)

Table 4. Interatomic distances pm, calculated with the powder lattice parameters of $Gd_5Pt_2In_4$

Gd1:	4	In1	321.9	Pt:	2	Gd3	285.7
	4	In2	334.3		1	In2	291.7
	2	Gd3	342.0		2	Gd2	295.0
	2	Gd1	367.6		2	Gd2	296.2
Gd2:	2	Pt	295.0		1	In1	297.1
	2	Pt	296.2		1	In2	333.4
	2	In2	333.2		2	Pt	367.6
	2	In1	333.6	In1:	1	Pt	297.1
	2	In2	339.0		2	Gd1	321.9
	2	Gd2	367.6		2	Gd3	322.6
	1	Gd3	370.7		1	In2	327.7
	1	Gd3	392.6		2	Gd2	333.6
Gd3:	2	Pt	285.7		2	Gd3	340.4
	2	In1	322.6		2	In1	367.6
	2	In2	330.7	In2:	1	Pt	291.7
	2	In1	340.4		1	In1	327.7
	1	Gd1	342.0		2	Gd3	330.7
	1	Gd3	356.8		2	Gd2	333.2
	2	Gd3	367.6		1	Pt	333.4
	1	Gd2	370.7		2	Gd1	334.3
	1	Gd2	392.6		2	Gd2	339.0

with the $Lu_5Ni_2In_4$ structure [5] was already evident from the powder patterns. The atomic parameters of isotypic $Sc_5Rh_2In_4$ [8] were then taken as starting atomic parameters and the $Gd_5Pt_2In_4$ structure was refined using SHELXL-97 (full-matrix least-squares on F_o^2) [9] with anisotropic atomic displacement parameters for all sites. As a check for the correct composition the occupancy parameters were refined in separate series of least-squares cycles. All sites were fully occupied within one standard deviation, and in the final cycles the ideal occupancies were assumed again. The refinements went smoothly to the residuals listed in Table 2. Due to the very small crystal size and the weak scattering power of the crystal, slightly higher residuals occurred. Nevertheless, the structure was unambiguously refined. Final difference *Fourier* syntheses revealed no significant residual peaks (Table 2). The positional parameters and interatomic distances are listed in Tables 3 and 4. Further details on the structure refinement may be obtained from: Fachinformationszentrum Karlsruhe, D-76344 Eggenstein-Leopoldshafen (Germany), by quoting the Registry No. CSD-417760.

Acknowledgements

We thank Dipl.-Chem. *F.M. Schappacher* for the work at the scanning electron microscope and Dr. *R.-D. Hoffmann* for the intensity data collection. This work was financially supported by the Deutsche Forschungsgemeinschaft.

References

[1] Kalychak YaM, Zaremba VI, Pöttgen R, Lukachuk M, Hoffmann R-D (2005) Rare Earth-Transition Metal-Indides. In: Gschneider KA Jr, Pecharsky VK, Bünzli J-C (eds) Handbook on the Physics and Chemistry of Rare Earths, Vol. 34, chapter 218. Elsevier, Amsterdam, p 1

[2] Galadzhun YaV, Pöttgen R (1999) Z Anorg Allg Chem **625**: 481

[3] Galadzhun YaV, Zaremba VI, Kalychak YaM, Davydov VM, Pikul AP, Stepień-Damm A, Kaczorowski D (2004) J Solid State Chem **177**: 17

[4] Tursina AI, Kurenbaeva ZM, Shepta DV, Nesterenko SN, Noël H (2006) Acta Crystallogr E **62**: i80

[5] Zaremba VI, Kalychak YaM, Zavalii PYu, Bruskov VA (1991) Krystallografiya **36**: 1415

[6] Pöttgen R, Gulden Th, Simon A (1999) GIT Labor Fachzeitschrift **43**: 133

[7] Yvon K, Jeitschko W, Parthé E (1977) J Appl Crystallogr **10**: 73

[8] Lukachuk M, Heying B, Rodewald UCh, Pöttgen R (2005) Heteroatom Chem **16**: 364

[9] Sheldrick GM (1997) SHELXL-97, Program for Crystal Structure Refinement, University of Göttingen

[10] Lukachuk M, Pöttgen R (2002) Z Naturforsch **57b**: 1353

[11] Lukachuk M, Hoffmann R-D, Pöttgen R (2004) Monatsh Chem **136**: 127

[12] Emsley J (1999) The Elements. Oxford University Press, Oxford

[13] Hoffmann R-D, Rodewald UCh, Pöttgen R (1999) Z Naturforsch **54b**: 38

[14] Hoffmann R-D, Pöttgen R (2001) Chem Mater **7**: 382

[15] Donohue J (1974) The Structures of the Elements. Wiley, New York

[16] Rodewald UCh, Zaremba VI, Galadzhun YaV, Hoffmann R-D, Pöttgen R (2002) Z Anorg Allg Chem **628**: 2293